



Multi-modal knowledge base generation from very high resolution satellite imagery for habitat mapping

Ioannis Manakos^{1*}, Eleanna Technitou², Zisis Petrou^{1,3}, Christos Karydas⁴,
Valeria Tomaselli⁵, Giuseppe Veronico⁵ and Giorgos Mountrakis⁶

¹Information Technologies Institute, Centre for Research and Technology Hellas,
Charilaou-Thermi Rd. 6th km, 57001, Thessaloniki, Greece

²Mediterranean Agronomic Institute of Chania, Makedonias 1, 73100, Chania, Greece

³The City College of New York, The City University of New York, NY10031, New York, USA

⁴Senior Researcher/ Consultant in Geomatics, Mesimeri, 57500, Epanomi, Greece

⁵Institute of Biosciences and BioResources (IBBR), National Research Council (CNR),
70126, Bari, Italy

⁶Department of Environmental Resources Engineering, State University of New York,
College of Environmental Science and Forestry, NY13210, Syracuse, USA

*Corresponding author, e-mail address: imanakos@iti.gr

Abstract

Monitoring of ecosystems entails the evaluation of contributing factors by the expert ecologist. The aim of this study is to examine to what extent the quantitative variables, calculated solely by the spectral and textural information of the space-borne image, may reproduce verified habitat maps. 555 spectral and texture attributes are extracted and calculated from the image. Results reached an overall accuracy of 65% per object, 76% per pixel, and 77% in reproducing the original objects with segmentation. Taking into consideration the large number of different habitats queried and the lack of any ancillary information the results suggest the discriminatory power of the finally selected attributes. Potential and limitations are discussed.

Keywords: Texture analysis, segmentation, EUNIS habitats, feature selection, random forest, ecosystem monitoring.

Introduction

In recent years, there has been an increasing interest in mapping and monitoring ecosystems and related services [Maes et al., 2012, 2016]. Mapping of ecosystems provides significant insight into their status and underlying functions, e.g. it allows the assessment of the effects of land-use change on the spatial distribution of environmental resources and the condition of the ecosystem services [Dickson et al., 2014]. Many organizations support the idea of ecosystem mapping as a core prerequisite towards ecosystem's protection. The "Mapping and Assessment of Ecosystem and their Services" (MAES) report states that "for the practical purposes of mapping and assessment, an ecosystem is considered at the scale of

habitat/biotope or landscape” [Maes et al., 2013]. This is how it is treated in this research as well.

According to MAES Technical Report [2014], mapping of ecosystems (and their services) is based on land cover datasets (e.g. CORINE land cover) and is largely dependent on their availability. The interpretation of such land cover data should be implemented on the basis of the European Nature Information System (EUNIS) habitat classification, in order to enrich the land cover information with more detailed information related with biodiversity. In fact, EUNIS has been recognized as an important standardizing tool for habitat classification in the EEA [Ichter et al., 2014] and as reference taxonomy for the establishment of a Red List of European habitats [Rodwell et al., 2013]. The definition of habitat according to EUNIS is: “a place where plants or animals normally live, characterized primarily by its physical features (topography, plant or animal physiognomy, soil characteristics, climate, water quality etc.) and secondarily by the species of plants and animals that live there” [Davies et al., 2004]. Habitat classification constitutes an integral part of EUNIS, developed and managed by the European Topic Centre for Nature Protection and Biodiversity (ETC/NPB in Paris) for the European Environment Agency (EEA) and the European Environmental Information Observation Network (EIONET) [Davies et al., 2004]. EUNIS provides a comprehensive typology for the habitats of Europe and its adjoining seas, acting as a common reference for habitats in the framework of the EU INSPIRE Directive [Ichter et al., 2014]. It provides cross-linkages to the habitat types listed in Annex 1 of the Habitat Directive [European Commission, 1992], attempting a link with ecosystems and ecosystem services.

Acting within this framework the cooperation of remote sensing researchers and experts for biodiversity assessment issues brings along important benefits in the science of ecology and the improvement of the monitoring techniques of the environment and its conservation status [Turner et al., 2003; Nagendra et al., 2012, 2014, 2015]. Ecosystem functions are linked to biodiversity, both directly and indirectly [Loreau et al., 2001; Costanza et al., 2006]. Apart from covering the urgent need for periodic and regular updates on land cover and habitat maps, attention is given to the objective reproducibility of the maps. A lot of different datasets, features, classification schemes and mapping methods have been developed and used to tackle aforementioned expectations and challenges [Bunce et al., 2008; Vanden Borre et al., 2011; Kosmidou et al., 2014]. A wide number of features have been extracted from remote sensing images and employed to enhance habitat mapping performance. Depending on the nature of the available data, they may range from spectral reflectance, backscatter coefficients, and 3D point clouds for passive radiometer, RADAR, and LIDAR data, respectively, to spectral band combinations, texture features, morphological, and topological features [Bock et al., 2005; Mishra et al., 2005; Boyd et al., 2006; Lucas et al., 2011; Cornforth et al., 2013; Petrou et al., 2014a; Adamo et al., 2014; Jin et al., 2014; Zhuang and Mountrakis, 2014].

The scope of this paper is to extract a feature knowledge base from a single multispectral very high resolution satellite image and examine its performance in discriminating EUNIS habitats both for their assigned category and their extent. No further ancillary knowledge is considered, in an effort to evaluate the potential of remotely sensed information content. Main aim is to quantitatively identify the support remote sensing may offer to ecologists

and mapping experts in their task to delineate processing-person indifferent reproducible boundaries and transition zones between habitats. Following the objective and framework set, a wide number of spectral and texture features are extracted from a very high resolution WorldView-2 (WV-2) image. Dimensionality reduction with a wrapper feature selection approach is applied to identify small subsets of features in the initial large set that best discriminate among habitat classes. Results are generated per object and per pixel. Finally, an iterative trial and error process is carried out to identify the capacity and limitations brought along with multilayer segmentation to support objective/ quantitative habitat boundaries' delineation.

Materials

The study area is a Natura 2000 site in Italy, namely Le Cesine (SCI IT9150032; SPA IT9150014). According to the World Wildlife Fund (WWF), Le Cesine is one of the best preserved wetlands of Southern Italy and the last surviving portion of what was once a vast wetland area ranging from Brindisi to Otranto. Le Cesine Nature Reserve is 380 hectares in size and it provides resting and breeding sites for many species of birds. This site is a coastal area, whose structure is mainly comprised of ponds, marshes and wet meadows, with a very high diversity in habitats and vegetation types [Tomaselli et al., 2011; Adamo et al., 2014].

On the basis of ground truth data by the National Research Council in Italy (CNR), and according to the Typology of Ecosystems proposed by Maes et al. (2013) as basic units for ecosystem mapping at European scale, there are two types of terrestrial ecosystems in the area of interest. The first one is the "sparsely vegetated land" and the second is the "marine inlets and transitional waters". All non-vegetated or sparsely vegetated habitats (naturally non-vegetated areas) were considered as sparsely vegetated land [Kosmidou et al., 2014]. Often these ecosystems are exposed to extreme natural conditions that might support particular species. They are open spaces with little or no vegetation (bare rocks, glaciers and dunes, beaches and sand plains). The marine inlets and transitional waters are ecosystems on the land-water interface under the influence of tides with salinity higher than 0.5% [European Commission, 2014]. They include coastal wetlands (saltmarshes, saline and intertidal flats), lagoons (highly restricted connection to open sea, and reduced, often relatively stable, salinity regime), estuaries and other transitional waters, fjords and sea lochs as well as embayment [European Commission, 2014]. Table 1 analytically describes the 21 different categories of EUNIS description evident in Le Cesine.

Table 1 - Le Cesine categories according to the EUNIS classification (The “Numbers” column is the representative number of each habitat to facilitate their use in the text, “EUNIS code” represents the codes of each habitat according to the EUNIS classification, “Number of polygons” and “Number of pixels” represent the number of polygons and pixels assessed for each habitat, respectively, in the study area, and “EUNIS description” represents the name of each habitat according to EUNIS).

<i>Number</i>	<i>EUNIS code</i>	<i>Number of polygons</i>	<i>Number of pixels</i>	<i>EUNIS description</i>
1	A2.522	40	6946526	Mediterranean <i>Juncus maritimus</i> and <i>Juncus acutus</i> salt marshes
2	A2.526	5	392	Mediterranean saltmarsh scrubs
3	A2.551	19	3543	Salicornia, Suaeda and Salsola pioneer saltmarshes
4	B1.1	5	20081	Sand beach driftlines
5	B1.31	29	26600	Embryonic shifting dunes
6	B1.63	34	6882	Dune <i>Juniperus</i> thickets
7	C2	4	20155	Surface running waters
8	C3.421	3	2321	Short Mediterranean amphibious communities
9	D5.1	38	172007	Reedbeds normally without free standing water
10	D5.24	169	268267	Fen <i>Cladium mariscus</i> beds
11	E1.313	14	2228	Mediterranean annual communities of shallow soils
12	E1.6	44	182154	Subnitrophilous annual grassland
13	F5.51	12	16915	Thermo Mediterranean brushes, thickets and heath garrigues
14	F5.514	141	197704	Lentisc brush
15	F6.2C	30	159006	Eastern <i>Erica</i> garrigues
16	G2.91	33	147003	<i>Olea europaea</i> groves
17	G3.F1	57	406081	Native conifer plantations
18	I1.3	5	11370	Arable land with unmixed crops grown by low intensity agricultural methods
19	J2.1	12	6273	Scattered residential buildings
20	J4.2	25	22983	Road networks
21	X03	41	281609	Brackish coastal lagoons

For the area of interest, a WV-2 image (Fig. 1) with a total of 8 bands was used for the analysis, in particular: Coastal (400-450 nm), Blue (450-510 nm), Green (510-580 nm), Yellow (585-625 nm), Red (630-690 nm), Red-Edge (705-745 nm), Near Infrared 1 (NIR-1) (770-895 nm), and NIR-2 (860-1040 nm) bands. For this study the panchromatic band was not used. The spatial resolution of the WV-2 image was 2 m after the pre-processing applied for georeferencing, co-registration, orthorectification and calibration in Top-of-Atmosphere reflectance values.

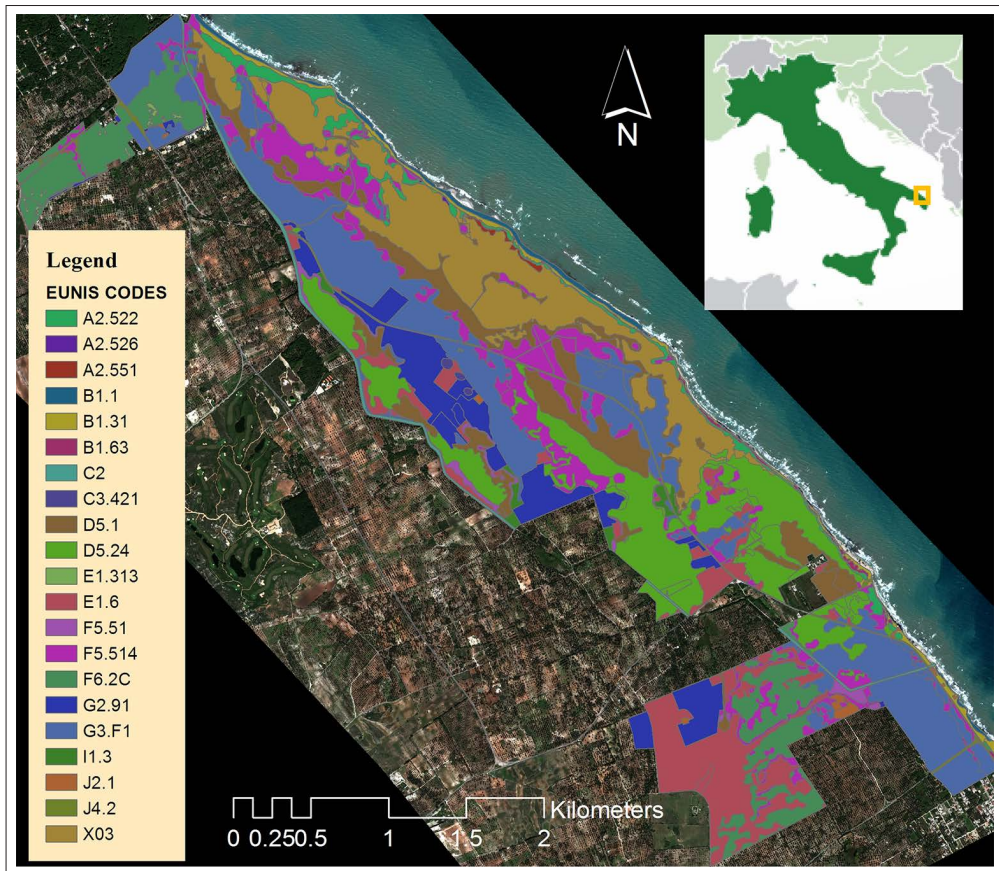


Figure 1 - Location of the area of interest, the WorldView-2 clipped image and the EUNIS categories.

CNR supported this research by offering i) a plethora of data specifying the land cover classes, which were used as segmentation layers in order to split the image into polygons/objects for this analysis, and ii) object-based information about the ecosystems on the ground according to the EUNIS system (Fig. 1). The latter was utilized as the ground truth information for this study. In particular, the data preparation by CNR included digitizing the thematic maps of the study site in ArcGIS 10.2 from recent colour orthophotos in combination with topographical maps (source: SIT-Puglia, <http://www.sit.puglia.it/>). Natural and semi-natural landscape elements were first defined as vegetation types on a

1:5,000 scale. This vegetation map represented the baseline position for natural and semi-natural types. Vegetation units were, thus, reclassified in EUNIS habitat types (level III and IV). As for anthropogenic (agricultural and artificial) types, they were directly assigned to EUNIS types. Maps were validated by in-field campaigns carried out in 2011-2013 to verify presence and distribution of both artificial and natural and semi-natural habitat types. Information on vegetation composition and structure, as well as agricultural practices or land use, was also collected. Such information, geocoded by GPS, was integrated into a GIS geo-database and allowed an accurate definition of some types.

Methods

The proposed methodology for this research is applied in two stages (Fig. 2):

- The first stage deals with the extraction of a wide number of spectral-based and texture features, and the selection of an effective feature subset, able to characterize and discriminate among different habitat classes. The features are extracted using as object boundaries the ones indicated by the units of the EUNIS thematic layer. A number of texture and spectral layers are derived by the WV-2 satellite image and are expressed as object attributes through a set of statistic measures. Then, wrapper-based feature selection is performed to select a small feature set able to be used for the classification of habitat classes.
- The second stage uses the features of the selected subset to provide a segmentation of the WV-2 imagery that accurately distinguishes the extent and boundaries of the habitat patches. Here, the object boundaries dictated by the ground truth thematic layer are considered unknown and are used solely for final performance evaluation. Two commonly used approaches are examined, a per-pixel classification and an object-based segmentation. The former used training sample pixels from the known objects to reproduce classes and their boundaries, while the latter is utilized and analyzed solely for its segmentation ability to reproduce classes' boundaries, not entering to any classification processing.

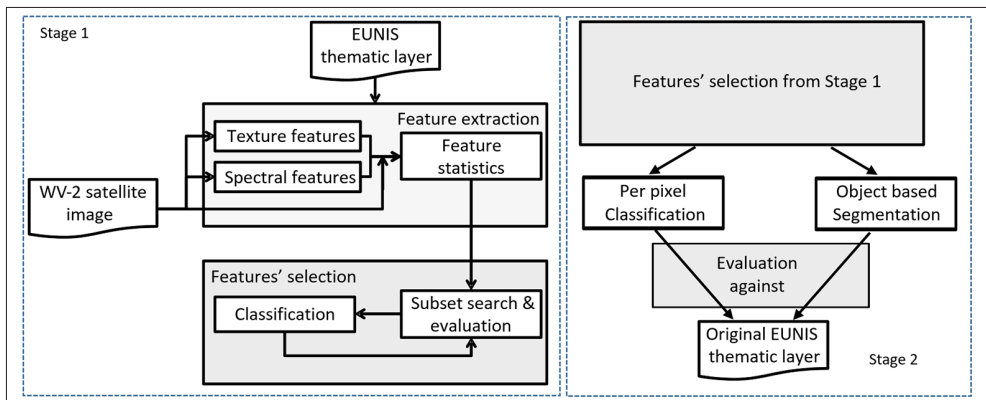


Figure 2- Workflow of the applied methodology.

Texture feature extraction

The texture feature analysis was performed by applying co-occurrence measurements in ENVI 5.0 [Zengeya et al., 2012] with the use of co-occurrence filtering. Each feature was extracted for each band in order to specify a large set of unique characteristics for each polygon and habitat. They represent extensive differences of gray tone in the image and provide spatial information by computing several angular relationships and distances between neighboring resolution cell pairs on the image [Haralick et al., 1973]. The selected texture features for this study are homogeneity, contrast, the second moment, entropy, correlation, and variance. The selection was based on related literature for land cover mapping, among which,

- Adamo et al. [2014] supported that entropy is characterized as the most suitable to represent the height of the trees, while when it is combined with variance, it can show the structure of the vegetation;
- Kayitakire et al. [2006] referred to correlation and entropy as the most relevant when analysing 6m spatial resolution optical images for land cover classification;
- Franklin et al. [2001] showed that homogeneity was more operative than the first-order variance in distinguishing age classes of some forests;
- Mohanaiah et al. [2013] suggested that the angular second moment is high when the image has very high homogeneity or when pixels are very similar.

Window sizes of 5×5 and 15×15 pixels were used for their calculation, shown to perform well with very high resolution images [Kayitakire et al., 2006].

Spectral indices calculation

Spectral indices aim to highlight certain spectral properties of habitats that may assist their characterization and discrimination. The following indices were used in this study:

- the Normalized Difference Vegetation Index (NDVI), which is a combination of band 5 (red band) and band 8 (NIR-2); more specifically it is equal to $(\text{band5} - \text{band8}) / (\text{band5} + \text{band8})$ of the WV-2 image;
- the Normalized Difference Soil Index (NDSI), a combination of the green (band 3) and the yellow (band 4) bands, more specifically equal to $(\text{band3} - \text{band4}) / (\text{band3} + \text{band4})$. NDSI determines the areas, where the soil is the dominant background or foreground material [Wolf, 2010];
- the Non-Homogeneous Feature Difference (NHFD), which is used to identify areas with human-made background [Wolf, 2010]. NHFD is calculated by dividing the difference of the coastal band from the red edge band by their sum $((\text{band6} - \text{band1}) / (\text{band6} + \text{band1}))$;
- the Difference Vegetation Index, calculated by subtracting the red from the near infrared band $(\text{band7} - \text{band5})$. In contrast with NDVI, DVI does not deal with the difference of the reflectance and the radiance caused by the atmosphere and the shadows; however, it is used to determine the vegetation and differentiate the soil and vegetation [Darvishzadeh et al., 2006];
- the Simple Ratio Index (SRI) is used, taking high values for vegetation and low ones for soil, ice and water. It also indicates the amount of vegetation and reduces the effects of atmosphere and topography $(\text{band7} / \text{band5})$ [Darvishzadeh et al., 2006];
- the Normalized Difference Water Index (NDWI) as a measure of water content in

vegetation canopies [Gao, 1996]. It is less sensitive than NDVI and is calculated by the ratio of the difference of the NIR-2 from the coastal band to their sum, $(\text{band8}-\text{band1})/(\text{band8}+\text{band1})$;

- the Optimized Soil Adjusted Vegetation Index (OSAVI) for agricultural monitoring, which is calculated as follows: $\text{OSAVI} = (1.5 \cdot (\text{band7}-\text{band5})) / (\text{band7}+\text{band5}+0.16)$ [Steven, 1998].

Estimation of statistical properties

The statistical analysis was based on the mean, the standard deviation, the minimum (min), the maximum (max), and the median of the pixels of each polygon. All these statistical properties were calculated for each polygon of each habitat, each index and each texture feature in the R programming language. In order to store all these data, matrices of all the variables were created and in the end were combined in a new data frame. This combination produced a big table for each polygon, containing all its values from every different band, band combination and texture feature in order to be used in the following processes. In total, each polygon is characterized by 555 features: five statistical values for i) the eight original WV-2 spectral bands, ii) the seven spectral indices, and iii) the six texture measures calculated for each band and for two window sizes.

Feature selection

A wide number of dimensionality reduction techniques have been proposed and employed in remote sensing datasets to decrease the feature space, including both transformation-based and feature selection techniques. Transformation-based techniques alter the original feature space, e.g. by applying linear or non-linear re-projections of the features to a new space of lower dimension than the original one [Gormus et al., 2012; Mahrooghy et al., 2012; Liu et al., 2014; Petrou et al., 2014b; Falco et al., 2015]. Feature selection methods, on the contrary, reduce the original feature space by removing entire features, applying no transformation to the remaining ones. The aim is to identify a high performing subset of features, reducing in parallel the processing cost of feature extraction and analysis processes. Features may be selected randomly, intuitively or based on literature review, or by following more sophisticated filter and wrapper approaches. Although not directly linked to the classification process, filter feature selection has proven effective in removing redundant information and provided subsets outperforming the full feature sets in classification accuracies, including even 3% of the original features [Petrou et al., 2015]. Wrapper approaches can use the same or similar search algorithms, but, contrary to filter feature selection algorithms, the evaluation of the feature subsets is linked with the learning scheme applied afterwards, e.g. is performed by evaluating directly the classification performance of each candidate subset [Vaiphasa et al., 2005; Chan and Paelinckx, 2008]. Wrapper approaches are usually more processing resources demanding than filter approaches, but have compared favorably to filter approaches since they are directly focused on optimizing the learning process outcome [Kohavi and John, 1997].

In this study, since the aim is to provide a feature subset optimizing the habitat classification performance, a wrapper feature selection approach is followed to identify subsets of the full feature set with high habitat classification performance. The wrapper approach consists

of a search and an evaluation algorithm, the former searching within the full feature set and forming candidate subsets and the latter evaluating the classification performance of these subsets. As far as the search method is concerned, exhaustive search would result in the evaluation of $2^{555}-1$ non-empty feature sets. Instead, a heuristic approach is employed, best-first [Hall, 1999], searching for the optimum subset among a restricted number of evaluated ones, in order to reduce the computational cost. Best-first performs a greedy search allowing backtracking, running iteratively and adding or removing one feature from the formed feature subset at each step. After each step, the feature set is evaluated by performing supervised habitat classification of the polygons. A random forest [Breiman, 2001] is used as a classifier, whereas the results are evaluated with 10-fold cross validation [Xu et al., 2014]. The process continues in the same manner, until either the entire feature set is searched or a termination criterion is met. In this study, the search is terminated, if no change in best feature subset is applied after a number of consecutive loops of feature expansion [Petrou et al., 2015].

Per pixel Classification

The per pixel classification took place using the support vector machine (SVM) classifier. SVMs are a popular choice in remote sensing classification with plethora of works, with a recent review available [Mountrakis et al., 2011]. Furthermore, SVMs have shown the highest classification potential, along with backpropagation neural networks, in a meta-analysis study of 15,000 published works in top tier remote sensing journals [Khatami et al., 2016]. In this application a range of training sample sizes was tested to allow custom decision making per application needs. The training and testing samples were selected using an unstratified random sampling protocol. The SVM algorithm was a collection of multiple binary SVM classifiers and implemented in Matlab. The parameter C that controls the maximum penalty imposed on margin-violating observations was optimized using a grid search. The Kernel scale was optimized using a built-in heuristic search function. The Kernel function was set to a Gaussian function (also referred as RBF). The classification product was further processed using a majority filter of varying size (5x5, 7x7, 9x9, 11x11) and the best performing algorithm (highest overall accuracy) was selected on a testing dataset of 20000 points for each training sample size. Accuracy results are reported on the entire wall-to-wall map. While there is overlap between the calibration datasets and the wall-to-wall map statistics the influence is negligible due to the large size of the map (>2 million pixels).

Image Segmentation

Image segmentation is the procedure of image object creation, resulting from image division into spatially continuous, disjoint and homogeneous regions [Blaschke, 2004]. Image objects are intended to be serving as information carriers and building blocks for classification or further segmentation processes. In this sense, the best segmentation result is the one that provides optimal information for further processing [Benz et al., 2004]. The current WV-2 image segmentation was examined towards the most possible accurate reproduction of the EUNIS habitat boundaries, using solely a layer stack of sixteen texture and spectral features (those resulted from the wrapper feature selection) without

incorporation of any ancillary data.

There are several approaches in categorising image segmentation algorithms [Dey et al., 2010], with the following being the most prevalent [Ohlander et al., 1978; Haralick and Shapiro, 1985]:

- Point-based algorithms, where a histogram is computed from all the image pixels and the peaks and valleys in the histogram are used to locate the clusters; e.g. *k*-means method [Barghout and Sheynin, 2013] or histogram thresholding [Shapiro and Stockman, 2001]. Point-based algorithms are known to be -by default- quite simplified approaches for mapping ecosystems, which are characterized by a big variety of biophysical parameters;
- Region-splitting algorithms, where large segments are divided into smaller units when the segments are not homogeneous enough, e.g. Quadtree methods [Horowitz and Pavlidis, 1974]. These methods are expected to bias the shape of the objects in homogeneous areas, therefore they are not always appropriate for large scales (in comparison to the pixel size). If smaller scales are opted, then segments need a round of manual or automated merging. If not used as an automated mapping process, it can be seen as supportive to visual interpretation;
- Edge-detection algorithms, where edges are regarded as boundaries between image objects located where changes in values of representativeness occur. Among the edge-detection methods [Kimmel, 2003], watershed algorithms alone are reported to result in over-segmentation [Gonzalez and Woods, 2008]. This is not desirable for ecosystems, which are used to contain large amount of heterogeneity. In addition to that, smoothing the image before applying a watershed algorithm, in order to reduce the local minima, thus avoiding over-segmentation, is considered to be a prerequisite. Generally, they are complicated methods, efficient when a single class is targeted;
- Region-growing algorithms, which aggregate pixels starting with a set of seed points, while the neighbouring pixels are joined through a continuous process until a certain threshold is reached. These algorithms [Blaschke, 2004] seem more efficient to achieve realistic shapes -but normally, they are quite intuitive and need a lot of trials; also, under-segmentation is a common problem in region-growing.

A region-growing algorithm, namely the Multiresolution Segmentation (also known as Fractal Net Evolution Approach, FNEA), supported by eCognition Developer software ®, was used for the segmentation of the WV-2 image. The most determining parameter influencing the desired object size in Multiresolution Segmentation is the scale parameter, while the object's geometry is influenced by the ratio of the shape to colour factor and the ratio of compactness to smoothness factor [Baatz et al., 2002].

Generally, the accuracy of produced objects fitting with reference EUNIS polygons, is expected to improve as scale decreases; the far extreme of this assumption is the production of one-pixel-sized objects, which would not be split between EUNIS polygons. On the other hand, an increased number of objects will also increase required post processing efforts in the framework of a following classification task. It is obvious, therefore, that an 'ideal segmentation' would be that of producing a number of objects equal to the number of reference objects, provided that they would also fit them geometrically.

For assessing the discrepancy between mapped and reference objects, the fuzzy set theory was employed [Kosko, 1993]. Hofmann et al. [2011] consider fuzzy logic theory appropriate

for object-based image analysis methodologies. Dey et al. [2010] suggest use of fuzzy models to represent ambiguity of region boundaries. Moreover, other more conventional measures (see for example Clinton et al. [2010]), were not found appropriate for irregular objects such as habitats. Fuzzy set theory follows a multivalued logic incorporating all possible outcomes in an observation, beyond the standard bivalent logic (i.e. a Boolean logic), common in conventional computing [Dutta et al., 2012].

Among several measures (or indicators) available for comparing segmentation and reference objects (polygons), volume similarity is considered to be easy in implementation and intuitive in meaning, as it is based on summing up true/false positives and negatives through overlap scores [Konukoglu et al., 2012]. Here, the segmentation object extent was employed as a volume similarity index, in order to provide a quantitative value of fuzzy membership of every object belonging to a single EUNIS reference polygon. Precisely, every object was assigned its full extent as a score (value=1) when belonging to a single reference polygon, whereas only the largest part of its extent was assigned to a single reference polygon when it was split between more than one polygons (value<1). The exact fuzzy scoring function was defined as follows:

$$M = \frac{O_i}{O_e} \quad [1]$$

M : score of object O in fitting a reference polygon in the interval $[0,1]$, O_i : extent of object O found inside a single reference polygon, O_e : extent of the entire object O . Correct extents were summed up for the entire area and per class, to provide score values in terms of extent percentages. M score could be seen as equivalent to ‘SimSize’ measure, introduced by [Zhan et al., 2005], only when the mapped object is completely within a reference object. Especially for the ‘ideal segmentation’ case, geometric accuracy of the objects was assessed. Considering that every object was expected to fit a single reference polygon, the following object properties were employed as geometric measures of the targeted fitness [Definiens, 2004]: Length; Width; Length/width; Asymmetry (as a measure of being invariant to a transformation); roundness (as a measure of how closely the shape of an object approaches that of a circle); elliptic fit; rectangular fit; shape index (as a measure of object’s outline complexity ranging from 1 to $+\infty$, with the smallest value [1] corresponding to an ideal square shape).

The results of all geometric measures derived from all the segmented objects and the reference polygons were compared statistically per geometric measure (namely, for mean, standard deviation, coefficient of variation, minimum, and maximum values). Ratio of statistical values of segmented objects over the same statistic of reference polygons was used as an index of similarity.

Results and discussion

Feature evaluation

The selection of the highest performing feature subsets was done by considering in the wrapper approach the entire study area, i.e. 760 polygons belonging in 21 EUNIS habitat

classes. A number of two and five loops without change in the best feature subset provided the best results among the tested best-first termination criterion parameters. In classification, random forests with 100 trees provided higher performance compared with random forests with less trees and comparable performance to random forest with more trees, with less processing requirements.

Table 2 reports the achieved classification accuracies of the feature subsets selected by best-first with five ('BF5') and two ('BF2') consecutive loops of no change to the best feature set as the termination criterion. They are compared with the accuracy from the full feature set ('ALL'). All feature sets were classified with the random forest with 100 trees and assessed with 10-fold cross-validation. BF5 set was selected as the one with the highest overall accuracy (OA) in classification - i.e. the ratio of correctly classified polygon to the total number of polygon - of nearly 65.5% and Cohen's kappa coefficient [Cohen, 1960] for 21 classes. BF2 was selected as a high performing subset with almost the minimum number of features among all experiments. The difference in OA between BF2 and BF5 is around 2%; however, BF2 set employs less than half the number of features employed in BF5, thus, it provides an even further gain in processing requirements for both feature extraction and classification. Both feature sets outperformed the accuracy achieved by the full feature set, employing 6.1% and 2.9% of the number of features of the full feature sets. The result suggests that a large amount of redundant and irrelevant information exists in the full feature set and has been successfully removed under the feature selection.

Table 2 - Best habitat classification performance of two features subsets selected by the wrapper approach.

Feature set	Number of feature	OA%	kappa
BF5	34	65.39%	0.6019
BF2	16	63.16%	0.5764
ALL	555	61.05%	0.5515

The features included in the subsets resulting from the BF5 and BF2 high performing approaches are listed in Table 3. As observed, there is a wide heterogeneity on the type of selected features. All categories of features, i.e. reflectance bands, spectral indices, and texture values, are represented in the two subsets, as well as both texture estimation windows - 5×5 and 15×15 pixels - and all statistics measures. This suggests that the selection process favors feature heterogeneity, where each feature offers separate discriminatory characteristics. As shown in previous studies [Topouzelis and Psyllos, 2012; Petrou et al., 2015], the derived subsets from a feature selection process do not necessarily include the highest performing individual features, but instead, favor features whose information is supplementary with little correlation. It is noteworthy that even though solely optical satellite image extracted features are employed in this study, the classification accuracies achieved are comparable to studies embedding ancillary data sources. For instance, rule-based habitat classifiers employing a limited number of remote sensing-derived features

but land cover prior knowledge and LIDAR data [Adamo et al., 2014; Petrou et al., 2014a], achieved overall accuracies around 70%, when applied in the same area. This demonstrates the potential of very high resolution optical data in habitat discrimination and the importance of the selection of appropriate features.

Table 3 - Features included in the selected high performing feature subsets. (The first part of each feature name represents the statistics measure (e.g. median, mean, minimum), followed by the type of feature, i.e. a reflectance band, e.g. 'B1', a spectral index, e.g. 'DVI', or a texture feature, e.g. 'B2Entr5' representing entropy calculated in band 5 with a 5×5 pixels window).

Feature set	Selected features
BF5	medianB4, meanB5, medianDVI, meanNDWI, medianNDWI, meanNHFD, sdNHFD, medianB1SecMom5, minB1SecMom5, medianB2Varian5, minB2Entr5, medianB5Varian5, maxB5Cor5, minB8SecMom5, maxB8Cor5, minB1Contr15, medianB1SecMom15, sdB2Contr15, minB2Varian15, sdB3SecMom15, meanB3Entr15, minB3Hom15, medianB4Varian15, minB4Hom15, maxB5Contr15, sdB5SecMom15, medianB5Cor15, sdB6Contr15, meanB6Cor15, minB7SecMom15, maxB7Entr15, meanB8Contr15, sdB8Entr15, medianB8Hom15
BF2	meanB5, medianDVI, medianNDWI, medianNHFD, meanB1Hom5, minB2Entr5, medianB7Entr5, maxB8Cor5, medianB2SecMom15, medianB4Varian15, medianB5Entr15, maxB5Entr15, minB5Cor15, maxB5Hom15, sdB6Contr15, meanB6Entr15

Table 4 draws the confusion matrix for the classification of the BF2 feature set. High accuracies were achieved by 6 classes, namely class B1.1 (4) (100% accuracy), class B1.31 (5) with 21 polygons, class B1.63 (6) with 23 polygons, class D5.24 (10) with 144 polygons, class F5.514 (14) with 120, and class X03 (21) with 29 correctly classified polygons. As may be generally inferred, classes with a large number of polygons have resulted in high producer's and user's accuracies. Average to low accuracies were reached by 3 classes, namely A2.551 (3), G2.91 (16), and G3.F1 (17), with more than half of the polygons correctly classified. Aforementioned show the discriminatory potential of remote sensing for the specific area and conditions in reproducing maps originally generated by experts. The limitations become obvious for classes, where remote sensing failed to perform at all, such as in cases of classes A2.526 (2), C2 (7), C3.421 (8) and I1.3 (18), or partially for the rest 8 classes with accuracies ranging from 8.3% to 42.5%.

Table 4 - Confusion matrix from the classification of the BF2 feature subset, as reported in Table 3.

		Prediction																							
		1	2	3	4	5	6	7	8	9	10	11	12	13	14	15	16	17	18	19	20	21	PA%		
Ground truth	1	17		1		2	2			3	5	1	2		5						2		42.5		
	2		0				1						1		2							1		0.0	
	3	1		10		4	2								1								1	52.6	
	4				5																			100	
	5	1		2	1	21	3				1													72.4	
	6	1				3	23								4		1	1					1	67.6	
	7							0							2	1					1			0.0	
	8								0				2		1									0.0	
	9	3									18	13			4									47.4	
	10	1				2	1		1	5	144		3	2	7		1					2	1	85.2	
	11	3							0		1	5			4								1	35.7	
	12	2								1	6		17	3	7	2	3				1	1	1	38.6	
	13										6		1	1	4										8.3
	14	2	1				4				6		1		120	1	1	3			1		1	85.1	
	15						2			1	1		1		15	8		2						26.7	
	16						1				7		2		5		17				1			51.5	
	17						3				1				20			33						57.9	
	18												3		1							1		0.0	
	19	1				2	1						2									4		2	33.3
	20					2	2					1			8		2					1	8	1	32.0
	21	3		1			2			2	4												0	29	70.7
UA(%)		48.6	0.0	71.4	83.3	58.3	48.9	-	0.0	60.0	73.8	71.4	48.6	16.7	57.1	66.7	68.0	86.4	-	50.0	50.0	78.4			
OA(%) :63.16; k :0.5764																									

Classification per pixel

The per pixel classification took place on the BF2 feature subset at varying training sample sizes. The results are reported in Figure 3. The optimal majority filter was identified as 11x11 for all sample sizes.

Results indicate a progressive increase in overall accuracy, reaching up to 76%, as the training sample increases. It is also evident that the majority filter offers accuracy improvements and it is suggested to incorporate this post-filtering process.

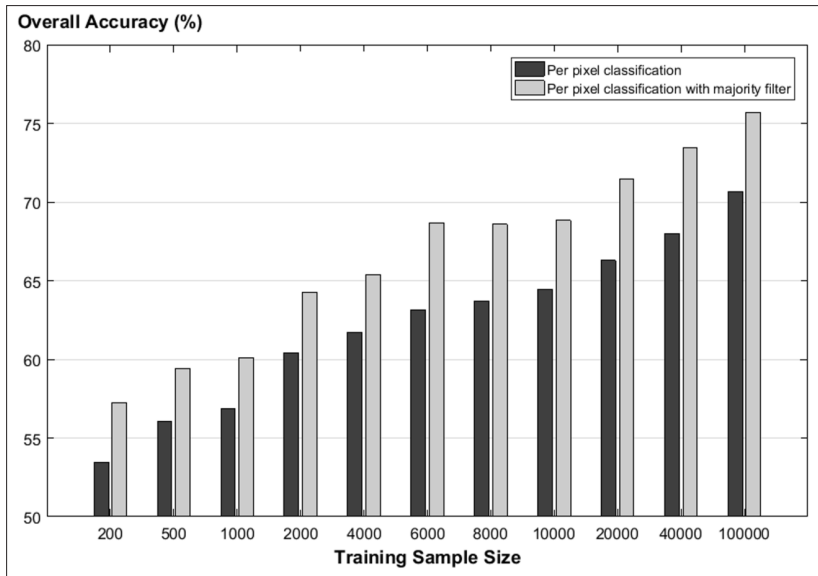


Figure 3 - Obtained accuracy for different training sample sizes.

Table 5 - User's and Producer's accuracies for a 6000 training sample size with majority filter.

Class	User (%)	Producer (%)	Description	Class	User (%)	Producer (%)	Description
1	66.8	29.9	Mediterranean (Medt.) salt marshes	11	-	0.0	Medt. annual shallow soils
2	-	0.0	Medt.saltmarsh scrubs	12	71.9	73.5	Subnitrophilous annual grassland
3	0.0	0.0	S.S.S. pioneer saltmarshes	13	29.3	1.7	Thermo Medt. bushes, thickets
4	81.2	72.9	Sand beach driftlines	14	48.9	39.7	Lentisc brush
5	42.5	78.7	Embryonic shifting dunes	15	76.1	46.0	Eastern Erica garrigues
6	48.8	2.1	Dune thickets	16	74.9	86.5	Olea europaea groves
7	79.6	10.5	Surface running waters	17	68.3	88.2	Native conifer plantations
8	-	0.0	Short Medt. amphibious	18	100.0	0.1	Arable land with unmixed crops
9	55.2	47.5	Reedbeds w/out standing water	19	94.2	2.4	Scattered buildings
10	67.3	81.3	Fen beds	20	44.3	1.0	Road networks
				21	88.3	92.8	Brackish coastal lagoons

The training sample size of 6000 with majority filtering was examined further as it strikes a balance between accuracy and reference data creation effort. Table 5 indicates large accuracy variability between classes, most notably the underperformance in salt marshes. Possible reasons of misclassifications may originate from the size and density of the spatial distribution of the polygons representing a class. For example, for class A2.551 the polygons are too small and really close to each other. Based on that it can be hypothesized that there are not polygons from this category included in the 6000 training sample size, however there were features, which were able to identify correctly this class. In the same way worked the classification of the road network (J4.2), which is basically many lines spread all over the area and since in the sample only a small part of these lines selected, it was impossible to have high accuracy. Furthermore, this category misclassified mostly with the F5.514 class, which is Lentisc brush, and this might have happened due to the fact that the Lentisc brush is widespread and abundant in thermo-Mediterranean and coastal meso-Mediterranean zones of the entire Mediterranean basin and the selection of such samples might be close to rail network and that’s why they have been misclassified.

Segmentation

First, the trend of produced object number vs. scale and colour/shape ratio was examined for scales ranging from 75 to 300 and two different colour/shape ratios: 0.1 and 0.3). The tests indicated a power-based function between scale and produced number of objects in both cases of colour/shape ratio (Fig. 4); in their work on a mixed agro-natural environment of Crete Island (Greece), Karydas et al. [2014] indicated a quadratic relation between scale and object size. Finally, a 0.3 shape/colour value was selected as most appropriate for the segmentation, as is considered to express better linear features in the habitat map, such as paths, channels, long transitional zones, or coastlines. Similarly, Karydas and Gitas [2011] have used a 0.2 shape/colour ratio for capturing linear features in Mediterranean agricultural landscapes.

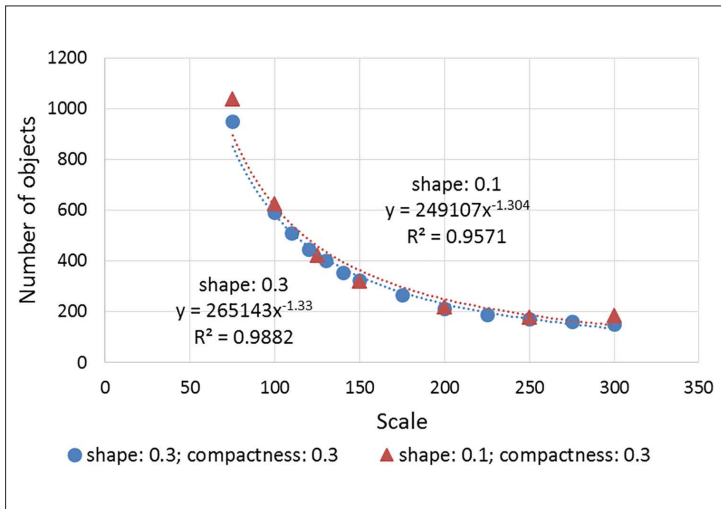


Figure 4 - Trend of number of objects vs. scale and shape/ colour ratio for different trials of the 16-feature layer stack.

From the object size vs. scale trend-graph, it is derived that a scale between 120 and 130 would result in a number of objects close to the number of reference polygons, thus, should be considered as ‘ideal segmentation’. Actually, the output of the 128-scale segmentation after removal of noisy objects (all objects smaller than 200 m²), was 408, which is very close to 417, i.e. the number of reference polygons. This number (417) results from the original 760 EUNIS polygons after spatially merging according to the EUNIS nomenclature. The threshold of 200 m² was determined visually, as the target of image segmentation is always to produce meaningful objects.

Mapping discrepancy of segmentation at the ‘ideal’ scale parameter (128) resulted in an overall accuracy of 76.9%, or 0.769 in terms of membership value in the range [0,1] (Fig. 5, Tab. 6). When scale parameter was decreased at 100, accuracy was increased to 80.4%; finally, at a 75 scale parameter, accuracy raised to 82.6%. These figures can be considered as encouraging, provided that good segmentation performance is a prerequisite for successful classification procedures.

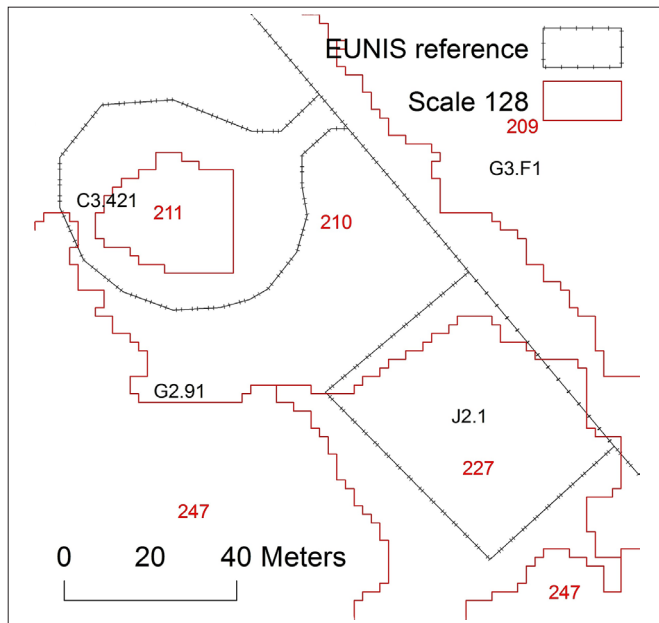


Figure 5 - A small subset of the Scale-128 segmentation layer with the reference polygons: polygon 211 is taken as correct by default; whereas polygon 227 will be taken as correct if its share inside J2.1 polygon is the largest share of this object, otherwise as wrong.

Going into more detail in the per-class accuracy figures, most classes show to improve their accuracy with lowering of the scale parameter, except class A2.551, which shows a significant decrease (from 60.8% to 48.8%). Notice, however, that the specific class contains only two polygons of quite limited extent. Another particular EUNIS class is B1.63, which shows null accuracy at 128 scale parameter, while raising to 50.9% accuracy at 75 scale. This fact can be explained by the extremely narrow polygons of the class.

Table 6 - Accuracy figures of object segmentation per EUNIS class at 128 scale parameter.

Class	Scale	128	76.9%	100	80.4%	75	82.6%
	Reference	Correct	Accuracy	Correct	Accuracy	Correct	Accuracy
A2.522	185,102	85,505	46.0%	100,468	54.3%	110,928	60.1%
A2.526	1,229	0	0.0%	0	0.0%	0	0.0%
A2.551	13,997	5,323	60.8%	5,052	36.1%	6,742	48.8%
B1.1	78,919	55,668	70.5%	58,278	73.8%	60,846	77.1%
B1.31	104,231	74,487	71.3%	66,975	64.3%	67,530	65.1%
B1.63	26,436	0	0.0%	5,405	20.4%	13,194	50.9%
C2	77,287	30,382	38.9%	29,841	38.6%	33,372	43.5%
C3.421	8,986	680	7.6%	680	7.6%	3,516	40.3%
D5.1	684,480	445,445	65.1%	480,350	70.2%	519,382	76.1%
D5.24	1,070,161	873,346	81.0%	912,615	85.3%	915,600	85.0%
E1.313	7,856	0	0.0%	0	0.0%	0	0.0%
E1.6	724,784	591,180	81.5%	616,906	85.1%	640,553	88.5%
F5.51	66,999	27,719	41.3%	28,904	43.1%	29,626	44.4%
F5.514	781,148	379,478	48.5%	421,867	54.0%	458,078	58.9%
F6.2C	632,451	530,368	83.8%	557,918	88.2%	556,769	88.1%
G2.91	585,279	545,183	93.1%	543,383	92.8%	545,470	93.4%
G3.F1	1,608,086	1,419,808	88.1%	1,437,796	89.4%	1,456,274	90.8%
I1.3	44,901	7,581	16.9%	10,270	22.9%	20,709	46.2%
J2.1	24,337	19,196	78.8%	17,867	73.4%	18,180	75.1%
J4.2	87,549	41,831	47.4%	47,905	54.7%	48,718	56.9%
X03	1,117,558	977,180	87.3%	1,032,053	92.3%	1,031,539	92.4%

Higher accuracies can generally be linked with EUNIS classes covering large extents through logarithmic equations with acceptable R^2 (0.5968, 0.7446, and 0.7290 for 128, 100, and 75 scale parameter, respectively) (Fig. 6).

For scales 128, 100, and 75, the produced number of objects was divided by the number of habitat polygons, i.e. 417 (segmentation objects/reference polygons), thus resulting in a measure of under- or over-segmentation (Fig. 7):

- Scale 128, resulting 408 objects; segmentation ratio: 0.97 (slight under-segmentation; the closest to 'ideal');
- Scale 100, resulting 590 objects; segmentation ratio: 1.41 (moderate over-segmentation);
- Scale 75, resulting 951 objects; segmentation ratio: 2.28 (significant over-segmentation).

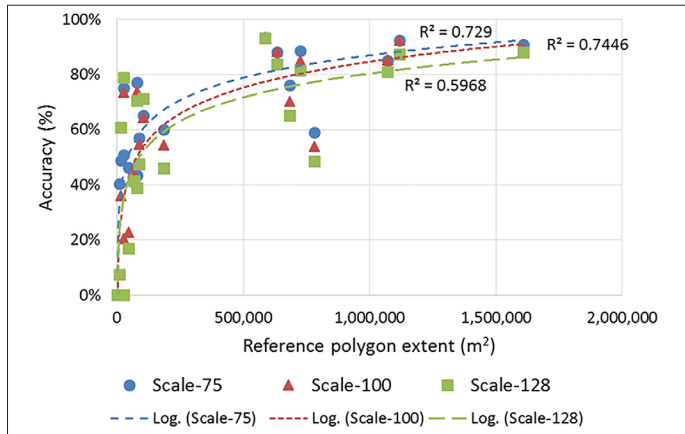


Figure 6 - Accuracy-extent figures for the different EUNIS classes per segmentation scale factor.

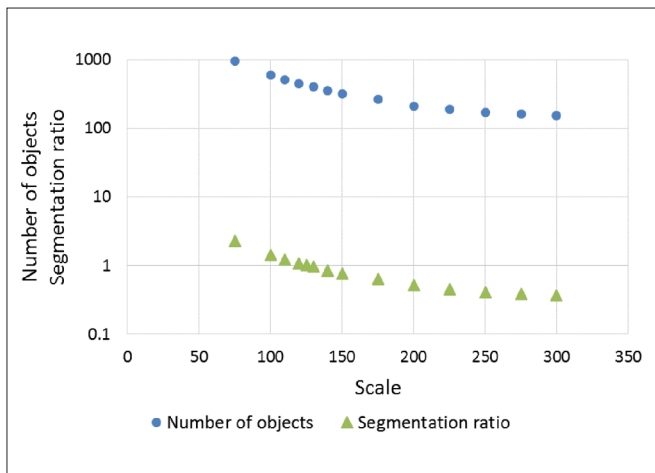


Figure 7 - A graph of segmentation ratio per scale factor - in parallel with the produced number of objects per scale.

Considering that scale 75 results in an accuracy increase by 5.7%, compared to the ‘ideal scale’, one could suggest this scale for implementation, provided that post-processing of the output polygons could be supported. Therefore, the ‘ideal scale’ should be considered as such, only by taking into account that no-processing is allowed.

Comparison of the shape statistics derived from the segmented objects and the reference data, demonstrate significant average geometric similarity between segmentation results and EUNIS polygons (Tab. 7). More specifically, Roundness, Elliptic fit, Rectangular fit, and Shape index give very close Mean figures for the segmentation and the reference data (ratios of means of segmented objects over reference polygons, between 1.0 and 1.07), whereas Asymmetry shows to be little smaller for the segmentation outputs (ratio: 0.85). On the other hand, segmentation outputs seem to be longer and wider than the reference

polygons (ratios: 1.21 and 1.45, respectively), but cannot reach the correct Length/Width ratio, as this is found to be quite lower than in the reference polygons (ratio: 0.71). Finally, the Coefficient of Variation (CV) for the segmented objects shows to be quite lower than the reference for the simpler measures (Length, Width, and Length/Width), whereas is almost similar (or slightly higher) for the more complex measures (Asymmetry, Roundness, Elliptic fit, Rectangular fit, and Shape index).

Table 7 - Accuracy figures of object segmentation per EUNIS class at various scale parameters.

Type	Stats	Length	Width	L/W	Asymmetry	Roundness	Elliptic Fit	Rectangular Fit	Shape Index
Reference	MEAN	140.38	47.64	3.58	0.71	1.47	0.44	0.67	2.65
	STD	226.16	60.37	3.92	0.23	1.05	0.27	0.2	1.63
	CV	161%	127%	109%	32%	71%	61%	30%	62%
	MIN	11.76	2.94	1	0.07	0.15	0	0	1.1
	MAX	1988.53	573	34.14	0.99	10.19	0.93	0.96	15.67
Scale 128	MEAN	170.45	69.18	2.55	0.6	1.58	0.45	0.67	2.81
	STD	143.23	47.5	2.02	0.3	1.22	0.35	0.24	1.93
	CV	84%	69%	79%	50%	77%	78%	36%	69%
	MIN	1	1	1	0.01	0	0	0	0
	MAX	1029.57	231	17.01	0.99	8.54	1	1	9.37
Ratio	MEAN	1.21	1.45	0.71	0.85	1.07	1.02	1.00	1.06
(Segm/Ref)	STD	0.63	0.79	0.52	1.30	1.16	1.30	1.20	1.18
	CV	0.52	0.54	0.72	1.54	1.08	1.27	1.20	1.12
	MIN	0.09	0.34	1.00	0.14	0.00	1.00	1.00	0.00
	MAX	0.52	0.40	0.50	1.00	0.84	1.08	1.04	0.60

Concluding remarks and outlook

Summarizing the results (Tab. 8), one may notice that given the best discriminating remote sensing extracted features (Tab. 3), a segmentation of the habitat classes may be successful for 9 classes (over 70% fit to reality and 420 polygons), the per pixel classification with no further information may be satisfactory for 7 classes (over 72% compliance with the real situation on the ground, and 378 polygons), whereas the initial expert knowledge may be supported well for 6 classes (over 67% validation accuracy and 342 polygons). One may directly realize that around and more than half of the polygons could be identified as such with high accuracy. Looking closer at the possible drawbacks of the lower performing classes, at most low performing or failing cases, except for the Mediterranean *Juncus maritimus* and *Juncus acutus* salt marshes, the number of the polygons representing the class in the area (the training sample set respectively) and the area they cover for is pretty low. In addition to that, long features show low accuracy as well (0.71 ratio of segmented over reference polygons for length/width parameter). It may be inferred that - at least - the

benefit of the doubt may be shared, which means that more experiments for the lower performing classes shall be conducted at areas, where an adequate number of polygons per habitat class exists.

Table 8 - Segmentation and classification ranking of performance for the different classes, prioritizing in sequence the ranking of segmentation, per pixel classification and object re-classification solely by remote sensing extracted features according to Producer Accuracies at scale 128 (see Tab. 6), for 6000 training sample size (see Tab. 5) and from the BF2 feature subset (see Tab. 4), respectively.

Number	EUNIS code	Number of polygons	Number of pixels	EUNIS description	PA at scale 128	PA for 6000 training sample size	PA from BF2 feature subset
16	G2.91	33	147003	Olea europaea groves	93.1	86.5	51.5
17	G3.F1	57	406081	Native conifer plantations	88.1	88.2	57.9
21	X03	41	281609	Brackish coastal lagoons	87.3	92.8	70.7
15	F6.2C	30	159006	Eastern Erica garrigues	83.8	46	26.7
12	E1.6	44	182154	Subnitrophilous annual grassland	81.5	73.5	38.6
10	D5.24	169	268267	Fen <i>Cladium mariscus</i> beds	81	81.3	85.2
19	J2.1	12	6273	Scattered residential buildings	78.8	2.4	33.3
5	B1.31	29	26600	Embryonic shifting dunes	71.3	78.7	72.4
4	B1.1	5	20081	Sand beach driftlines	70.5	72.9	100
9	D5.1	38	172007	Reedbeds normally without free standing water	65.1	47.5	47.4
3	A2.551	19	3543	Salicornia, Suaeda and Salsola pioneer saltmarshes	60.8	0	52.6
14	F5.514	141	197704	Lentisc brush	48.5	39.7	85.1
20	J4.2	25	22983	Road networks	47.4	1	32
1	A2.522	40	6946526	Mediterranean <i>Juncus maritimus</i> and <i>Juncus acutus</i> salt marshes	46	29.9	42.5
13	F5.51	12	16915	Thermo Mediterranean brushes, thickets and heath garrigues	41.3	1.7	8.3
7	C2	4	20155	Surface running waters	38.9	10.5	0
18	I1.3	5	11370	Arable land with unmixed crops grown by low intensity agricultural methods	16.9	0.1	0
8	C3.421	3	2321	Short Mediterranean amphibious communities	7.6	0	0
6	B1.63	34	6882	Dune Juniperus thickets	0	2.1	67.6
11	E1.313	14	2228	Mediterranean annual communities of shallow soils	0	0	35.7
2	A2.526	5	392	Mediterranean saltmarsh scrubs	0	0	0

Even with the lack of expert knowledge existing remote sensing products and methods seem to have high discriminatory information content, which may be utilized and possibly synthesized to standardized procedures for habitat mapping. A further step to examine could be the provision of multiple class assignments as options to the expert to decide from. This may be considered upon agreement for its added value with the experts. After all decision making processes require for objective and quantitative support. Latter is driven by the need to support sustainable development towards the Biodiversity Targets for 2020, i.e. the need for development and implementation of relevant policies on water, climate, agriculture, forest, and regional planning [European Commission, 2014] in an as objective way as possible.

Acknowledgements

This work is supported and partially funded by the European Union's Horizon 2020 research and innovation programme under grant agreement No 641762, ECOPotential project.

References

- Adamo M., Tarantino C., Tomaselli V., Kosmidou V., Petrou Z.I., Manakos I., Lucas R.M., Múcher C.A., Veronico G., Marangi C., De Pasquale V., Blonda P. (2014) - *Expert Knowledge for Translating Land Cover/use Maps to General Habitat Categories (GHC)*. *Landscape Ecology*, 29 (6): 1045-1067. doi: <http://dx.doi.org/10.1007/s10980-014-0028-9>.
- Baat M., Benz U., Dehghani S., Heynen M., Holtje A., Hofmann P., Lingenfelder I., Mimler M., Sohlbach M., Weber M., Willhauck G. (2002) - *ECognition User's Guide*. Munich, Germany: Definiens Imaging GmbH, digital.
- Barghout L., Sheynin J. (2013) - *Real-world scene perception and perceptual organization: Lessons from Computer Vision*. *Journal of Vision*, 13 (9): 709-709. doi: <https://doi.org/10.1167/13.9.709>.
- Benz U.C., Hofmann P., Willhauck G., Lingenfelder I., Heynen, M. (2004) - *Multi-resolution, object-oriented fuzzy analysis of remote sensing data for GIS-ready information*. *ISPRS Journal of Photogrammetry & Remote Sensing*, 58 (3-4): 239-258. doi: <https://doi.org/10.1016/j.isprsjprs.2003.10.002>.
- Blaschke T. (2004) - *Object based image analysis for remote sensing*. *ISPRS Journal of Photogrammetry and Remote Sensing*, 65 (1): 2-16. <https://doi.org/10.1016/j.isprsjprs.2003.10.002>.
- Bock M., Xofis P., Mitchley J., Rossner G., Wissen M. (2005) - *Object-oriented methods for habitat mapping at multiple scales - Case studies from Northern Germany and Wye Downs, UK*. *Journal for Nature Conservation*, 13: 75-89. doi: <http://dx.doi.org/10.1016/j.jnc.2004.12.002>.
- Boyd D.S., Sanchez-Hernandez C., Foody G.M. (2006) - *Mapping a specific class for priority habitats monitoring from satellite sensor data*. *International Journal of Remote Sensing*, 27 (13): 2631-2644. doi: <http://dx.doi.org/10.1080/01431160600554348>.
- Breiman L. (2001) - *Random forests*. *Machine Learning*, 45: 5-32. doi: <http://dx.doi.org/10.1023/A:1010933404324>.
- Bunce R.G.H., Metzger M.J., Jongman R.H.G., Brandt J., de Blust G., Elena-Rossello R., Groom G.B., Halada L., Hofer G., Howard D.C., Kovář P., Múcher C.A., Padoa

- Schioppa E., Paelinx D., Palo A., Perez Soba M., Ramos I.L., Roche P., Skånes H., Wrbka T. (2008) - *A standardized procedure for surveillance and monitoring European habitats and provision of spatial data*. Landscape Ecology, 23: 11-25. doi: <https://doi.org/10.1007/s10980-007-9173-8>.
- Chan J.C.-W., Paelinckx D. (2008) - *Evaluation of Random Forest and Adaboost tree-based ensemble classification and spectral band selection for ecotope mapping using airborne hyperspectral imagery*. Remote Sensing of Environment, 112: 2999-3011. doi: <http://dx.doi.org/10.1016/j.rse.2008.02.011>.
- Clinton N., Holt A., Scarborough J., Yan L., Gong P. (2010) - *Accuracy Assessment Measures for Object-based Segmentation Goodness*. Photogrammetric Engineering & Remote Sensing, 76 (3): 289-299. doi: <https://doi.org/10.14358/PERS.76.3.289>.
- Cohen J. (1960) - *A coefficient of agreement for nominal scales*. Educational and Psychological Measurement, 20: 37-46. doi: <http://dx.doi.org/10.1177/001316446002000104>.
- Cornforth W., Fatoyinbo T., Freemantle T., Pettorelli N. (2013) - *Advanced Land Observing Satellite Phased Array Type L-Band SAR (ALOS PALSAR) to Inform the Conservation of Mangroves: Sundarbans as a Case Study*. Remote Sensing, 5: 224-237. doi: <http://dx.doi.org/10.3390/rs5010224>.
- Costanza R., Fisher B., Mulder K., Liu S., Christopher T. (2006) - *Biodiversity and ecosystem services: A multi-scale empirical study of the relationship between species richness and net primary production*. Ecological Economics, 61: 478-491. doi: <https://doi.org/10.1016/j.ecolecon.2006.03.021>.
- Darvishzadeh R., Atzberger C., Skidmore A.K. (2006) - *Hyperspectral vegetation indices for estimation of leaf area index*. International Institute for Geo-information Science and Earth Observation, pp. 1-6.
- Davies C.E., Moss D., Hill M.O. (2004) - *EUNIS Habitat Classification Revised 2004*. European Environment Agency European Topic Centre on nature protection and biodiversity, pp. 1-307.
- Definiens (2004) - *eCognition 4 User Guide*. Definiens, Munich, Germany.
- Dey V., Zhang Y., Zhong M. (2010) - *A review on image segmentation techniques with Remote Sensing perspective*. Proceedings ISPRS TC VII Symposium - 100 Years ISPRS, IAPRS, XXXVIII:Part 7A.
- Dickson B., Blaney R., Miles L., Regan E., van Soesbergen A., Väänänen E., Blyth S., Harfoot M., Martin C., McOwen C., Newbold T., van Bochove J. (2014) - *Towards a global map of natural capital: Key ecosystem assets*. UNEP World Conservation Monitoring Centre, pp. 1-40.
- Dutta D., Roy Chowdhury A., Bhattacharya U., Parui S. K. (2012) - *Lightweight User-Adaptive Handwriting Recognizer for Resource Constrained Handheld Devices*. Proceedings of Workshop on Document Analysis and Recognition, ACM Conference Proceedings Series, pp. 114-119. doi: <https://doi.org/10.1145/2432553.2432574>.
- European Commission (1992) - *Council Directive 92/43 EEC of 22.7.92*. Official Journal of the European Communities L. 206/7.
- European Commission (2014) - *Mapping and Assessment of Ecosystems and their Services*. European Union, pp. 1-82. doi: <http://dx.doi.org/10.2779/75203>.
- Falco N., Benediktsson J.A., Bruzzone L. (2015) - *Spectral and Spatial Classification of Hyperspectral Images Based on ICA and Reduced Morphological Attribute Profiles*.

- IEEE Transactions on Geoscience and Remote Sensing, 53: 1-18. doi: <http://dx.doi.org/10.1109/TGRS.2015.2436335>.
- Franklin S.E., Wulder M.A., Gerylo G.R. (2001) - *Texture analysis of Ikonos panchromatic data for Douglas-fir forest age class separability in British Columbia*. International Journal of Remote Sensing, 22 (13): 2627-2632. doi: <https://doi.org/10.1080/01431160120769>.
- Gao B.C. (1996) - *Normalized difference water index for remote sensing of vegetation liquid water from space*. Imaging Spectrometry, pp. 257-266. doi: [http://dx.doi.org/10.1016/S0034-4257\(96\)00067-3](http://dx.doi.org/10.1016/S0034-4257(96)00067-3).
- Gonzales R.C., Woods R.E. (2008) - *Digital Image Processing*. Pearson Education, Incorporation, New Jersey, 3rd edition.
- Gormus E.T., Canagarajah N., Achim A. (2012) - *Dimensionality reduction of hyperspectral images using empirical mode decompositions and wavelets*. IEEE Journal of Selected Topics in Applied Earth Observations and Remote Sensing, 5: 1821-1830. doi: <http://dx.doi.org/10.1109/JSTARS.2012.2203587>.
- Hall M.A. (1999) - *Correlation-based feature selection for machine learning*. Ph.D. dissertation, University of Waikato, Hamilton, New Zealand.
- Haralick R.M., Shapiro L.G. (1985) - *Image segmentation techniques*. Computer Vision, Graphics, and Image Processing, 29 (1): 100-132. doi: [https://doi.org/10.1016/S0734-189X\(85\)90153-7](https://doi.org/10.1016/S0734-189X(85)90153-7).
- Haralick R.M., Shanmugam K., Dinstein I (1973) - *Textural Features for Image Classification*. IEEE Transactions on Systems, Man and Cybernetics, SMC-3 (6): 610-621. doi: <https://doi.org/10.1109/TSMC.1973.4309314>.
- Hofmann P., Blaschke T., Strobl J. (2011) - *Quantifying the robustness of fuzzy rule sets in object-based image analysis*. International Journal of Remote Sensing, 32 (22): 7359-7381. doi: <https://doi.org/10.1080/01431161.2010.523727>.
- Horowitz S.L., Pavlidis T. (1974) - *Picture Segmentation by a Directed Split and Merge Procedure*. Proceedings ICPR, Denmark, pp. 424-433.
- Ichter J., Evans D., Richard D. (2014) - *Terrestrial Habitat Mapping in Europe: An Overview*. European Environmental Agency: Luxembourg.
- Jin H., Mountrakis G., Stehman S. (2014) - *Assessing integration of intensity, polarimetric scattering, interferometric coherence and spatial texture metrics in PALSAR-derived land cover classification*. ISPRS Journal of Photogrammetry and Remote Sensing, 98: 70-84. doi: <https://doi.org/10.1016/j.isprsjprs.2014.09.017>.
- Karydas C.G., Gitas I.Z. (2011) - *Development of an IKONOS image classification rule-set for multi-scale mapping of Mediterranean rural landscapes*. International Journal of Remote Sensing, 32 (24): 9261-9277. doi: <https://doi.org/10.1080/01431161.2010.551549>.
- Karydas C.G., Tompoulidou M., Kalaitzidis Ch., Gitas I.Z. (2014) - *Segmentation of a WorldView2 image for feature identification in highly heterogeneous environments*. South-Eastern European Journal of Earth Observation and Geomatics, 3 (2S): 717-720.
- Kayitakire F., Hamel C., Defourny P. (2006) - *Retrieving forest structure variables based on image texture analysis and IKONOS-2 imagery*. Remote Sensing of Environment, 102 (3-4): 390-401. doi: <http://dx.doi.org/10.1016/j.rse.2006.02.022>.
- Khatami R., Mountrakis G., Stehman S. (2016) - *A meta-analysis of remote sensing research on land-cover image classification processes: A guide for practitioners and*

- directions for future research*. Remote Sensing of Environment, 177: 89-100. doi: <https://doi.org/10.1016/j.rse.2016.02.028>.
- Kimmel R. (2003) - *Fast edge integration*. In *Level Set Methods and Their Applications in Computer Vision, Chapter 3*. Springer Verlag: NY. doi: https://doi.org/10.1007/0-387-21810-6_4.
- Kohavi R., John G.H. (1997) - *Wrappers for feature subset selection*. Artificial Intelligence, 97: 273-324. doi: [http://dx.doi.org/10.1016/S0004-3702\(97\)00043-X](http://dx.doi.org/10.1016/S0004-3702(97)00043-X).
- Konukoglu E., Glocker B., Ye D.H., Criminisi A., Pohl, K.M. (2012) - *Discriminative Segmentation-based Evaluation through Shape Dissimilarity*. IEEE Transaction on Medical Imaging, 31 (12): 2278-2289. doi: <https://doi.org/10.1109/TMI.2012.2216281>.
- Kosko B. (1993) - *Fuzzy Thinking: The New Science of Fuzzy Logic (PhD)*. Hyperion New York.
- Kosmidou V., Petrou Z., Bunce R.G.H., Múcher C.A., Jongman R.H.G, Bogers M.M.B., Lucas R.M., Tomaselli V., Blonda P., Padoa-Schioppa E., Manakos I., Petrou M. (2014) - *Harmonization of the Land Cover Classification System (LCCS) with the General Habitat Categories (GHC) classification system*. Ecological Indicators, 36: 290-300. doi: <http://dx.doi.org/10.1016/j.ecolind.2013.07.025>.
- Liu K., Liu L., Liu H., Li X., Wang S. (2014) - *Exploring the effects of biophysical parameters on the spatial pattern of rare cold damage to mangrove forests*. Remote Sensing of Environment, 150: 20-33. doi: <http://dx.doi.org/10.1016/j.rse.2014.04.019>.
- Loreau M., Naeem S., Inchausti P., Bengtsson J., Grime J.P., Hector A., Hooper D.U., Huston M.A., Raffaelli D., Schmid B., Tilman D., Wardle D.A. (2001) - *Ecology, Biodiversity and ecosystem functioning: Current knowledge and future challenges*. Science, 294: 804-808. doi: <https://doi.org/10.1126/science.1064088>.
- Lucas R.M., Medcalf K., Brown A., Bunting P., Breyer J., Clewley D., Keyworth S., Blackmore P. (2011) - *Updating the Phase 1 habitat map of Wales, UK, using satellite sensor data*. ISPRS Journal of Photogrammetry and Remote Sensing, 66: 81-102. doi: <http://dx.doi.org/10.1016/j.isprsjprs.2010.09.004>.
- Maes J., Egoh B., Willemen L., Liqueste C., Vihervaara P., Schagner J.P., Grizzetti B., Drakou E.G., La Notte A., Zulian G., Bouraoui F., Paracchini M.L., Braat L., Bidoglio G. (2012) - *Mapping ecosystem services for policy support and decision making in the European Union*. Ecosystem Services, 1: 31-39. doi: <http://dx.doi.org/10.1016/j.ecoser.2012.06.004>.
- Maes J., Liqueste C., Teller A., Erhard M., Paracchini M.L., Barredo J.I., Grizzetti B., Cardoso A., Somma F., Petersen J.E., Meiner A., Royo Gelabert E., Zal N., Kristensen P., Bastrup-Birk A., Biala K., Piroddi C., Egoh B., Degeorges P., Fiorina C., Santos-Martín F., Naruševičius V., Verboven J., Pereira H.M., Bengtsson J., Gocheva K., Marta-Pedroso C., Snäll T., Estreguil C., San-Miguel-Ayán J., Pérez-Soba M., Grêt-Regamey A., Lillebø A.I., Abdul Malak A., Condé S., Moen J., Czúcz B., Drakou E. G., Zulian G., Laval C. (2016) - *An indicator framework for assessing ecosystem services in support of the EU Biodiversity Strategy to 2020*. Ecosystem Services, 17: 14-23. doi: <http://dx.doi.org/10.1016/j.ecoser.2015.10.023>.
- Maes J., Teller A., Erhard M., Liqueste C., Braat L., Berry P., Egoh B., Puydarrieux P., Fiorina C., Santos F., Paracchini M.L., Keune H., Wittmer H., Hauck J., Fiala I., Verburg P.H., Conde S., Schagner J.P., San Miguel J., Estreguil C., Ostermann O., Barredo J.I.,

- Pereira H.M., Scott A., Laporte V., Meiner A., Olah B., Royo Gelabert E., Spyropoulou R., Petersen J.E., Maguire C., Zal N., Achilleos E., Rubin A., Ledoux L., Brown C., Raes C., Jacobs S., Vandewalle M., Connor D., Bidoglio G. (2013) - *Mapping and Assessment of Ecosystems and their services. Analytical framework for ecosystem assessments under Action 5 of the EU Biodiversity Strategy to 2020. Discussion paper - Final*. Publications office of the European Union, Luxembourg.
- Maes J., Teller A., Erhard M., Murphy P., Paracchini M.L., Barredo J.I., Grizzetti B., Cardoso A., Somma F., Petersen J.E., Meiner A., Royo Gelabert E., Zal N., Kristensen P., Bastrup-Birk A., Biala K., Romao C., Piroddi C., Egoh B., Fiorina C., Santos F., Naruševičius V., Verboven J., Pereira H., Bengtsson J., Kremena G., Marta-Pedroso C., Snäll T., Estreguil C., San Miguel J., Braat L., Grêt-Regamey A., Perez-Soba M., Degeorges P., Beaufaron G., Lillebø A., Abdul Malak D., Liquete C., Condé S., Moen J., Östergård H., Czúcz B., Drakou E.G., Zulian G., Lavalle C. (2014) - *Mapping and Assessment of Ecosystems and their services. Analytical framework for ecosystem assessments under Action 5 of the EU Biodiversity Strategy to 2020. 2nd report - Final*. Publications office of the European Union, Luxembourg.
- Mahrooghy M., Younan N.H., Anantharaj V.G., Aanstoos J.V. (2012) - *Enhancement of satellite precipitation estimation via unsupervised dimensionality reduction*. IEEE Transactions on Geoscience and Remote Sensing, 50: 3931-3940. doi: <http://dx.doi.org/10.1109/TGRS.2012.2189406>.
- Mishra D.R., Narumalani S., Rundquist D., Lawson M. (2005) - *High-resolution ocean color remote sensing of benthic habitats: a case study at the Roatan island, Honduras*. IEEE Transactions on Geoscience and Remote Sensing, 43 (7): 1592-1604. doi: <http://dx.doi.org/10.1109/TGRS.2005.847790>.
- Mohanaiah P., Sathyanarayana P., Gurukumar L. (2013) - *Image Texture Feature Extraction Using GLCM Approach*. International Journal of Scientific and Research Publications, pp.1-5.
- Mountrakis G., Im J., Ogole C. (2011) - *Support vector machines in remote sensing: A review*. SPRS Journal of Photogrammetry and Remote Sensing, 66 (3): 247-259.
- Nagendra H., Lucas R., Honrado J.P., Jongman R.H.G., Tarantino C., Adamo M., Maitora P. (2012) - *Remote sensing for conservation monitoring: Assessing protected areas, habitat extent, habitat condition, species diversity, and threats*. Ecological Indicators, pp. 45-59. doi: <http://dx.doi.org/10.1016/j.ecolind.2012.09.014>.
- Ohlander R., Price K., Reddy D.R. (1978) - *Picture Segmentation Using a Recursive Region Splitting Method*. Corny Graph. Image Process, 8: 313. doi: [https://doi.org/10.1016/0146-664X\(78\)90060-6](https://doi.org/10.1016/0146-664X(78)90060-6).
- Petrou Z.I., Kosmidou V., Manakos I., Stathaki T., Adamo M., Tarantino C., Tomaselli V., Blonda P., Petrou M. (2014a) - *A rule-based classification methodology to handle uncertainty in habitat mapping employing evidential reasoning and fuzzy logic*. Pattern Recognition Letters, 48: 24-33. doi: <http://dx.doi.org/10.1016/j.patrec.2013.11.002>.
- Petrou Z.I., Manakos I., Stathaki T., Tarantino C., Adamo M., Blonda P. (2014b) - *A vegetation height classification approach based on texture analysis of a single VHR image*. Proceedings of the 35th International Symposium on Remote Sensing of Environment, IOP Conference Series: Earth and Environmental Science, 17: 012210. doi: <http://dx.doi.org/10.1088/1755-1315/17/1/012210>.

- Petrou Z.I., Manakos I., Stathaki T., Múcher C.A., Adamo M. (2015) - *Discrimination of vegetation height categories with passive satellite sensor imagery using texture analysis*. IEEE Journal of Selected Topics in Applied Earth Observations and Remote Sensing, 8 (4): 1442-1455. doi: <http://dx.doi.org/10.1109/JSTARS.2015.2409131>.
- Rodwell J., Janssen J., Gubbay S., Shaminée J. (2013) - *Red List Assessment of European Habitat Types - A feasibility study*. Report for the EU Commission, DG Environment. Available online at: <https://circabc.europa.eu/d/a/workspace/SpacesStore/cafecf35-58c4-4e28-818d-876614ba4477/RDB%20Final%20Report%20Version%20DEF%20160413.pdf>.
- Shapiro L.G., Stockman C.G. (2001) - *Computer Vision*. New Jersey, Prentice-Hall, ISBN 0-13-030796-3, pp. 279-325.
- Steven M.D. (1998) - *The sensitivity of the OSAVI vegetation index to observational parameters*. Remote Sensing of Environment, pp. 49-60. doi: [http://dx.doi.org/10.1016/S0034-4257\(97\)00114-4](http://dx.doi.org/10.1016/S0034-4257(97)00114-4).
- Tomaselli V., Tenerelli P., Sciandrello S. (2011) - *Mapping and quantifying habitat fragmentation in small coastal areas: a case study of three protected wetlands in Apulia (Italy)*. Environmental Monitoring and Assessment, 184 (2): 693-713. doi: <http://dx.doi.org/10.1007/s10661-011-1995-9>.
- Topouzelis K., Psyllos A. (2012) - *Oil spill feature selection and classification using decision tree forest on SAR image data*. ISPRS Journal of Photogrammetry and Remote Sensing, 68: 135-143. doi: <http://dx.doi.org/10.1016/j.isprsjprs.2012.01.005>.
- Turner W., Spector S., Gardiner N., Fladeland M., Sterling E., Steininger M. (2003) - *Remote sensing for biodiversity science and conservation*. Trends in Ecology and Evolution, pp. 306-314. doi: [http://dx.doi.org/10.1016/S0169-5347\(03\)00070-3](http://dx.doi.org/10.1016/S0169-5347(03)00070-3).
- Vaiphasa C., Ongsomwang S., Vaiphasa T., Skidmore A., (2005) - *Tropical mangrove species discrimination using hyperspectral data: A laboratory study*. Estuarine, Coastal and Shelf Science, 65: 371-379. doi: <http://dx.doi.org/10.1016/j.ecss.2005.06.014>.
- Vanden Borre J., Paelinckx D., Múcher C.A., Kooistra L., Haest B., De Blust G., Schmidt A.M. (2011) - *Integrating remote sensing in Natura 2000 habitat monitoring: Prospects on the way forward*. Journal of Natural Conservation, 19: 116-125. doi: <https://doi.org/10.1016/j.jnc.2010.07.003>.
- Wolf A. (2010) - *Using WorldView 2 Vis-NIR MSI Imagery to Support Land Mapping and Feature Extraction Using Normalized Difference Index Ratios*. Digital Globe, pp. 1-13 doi: <http://dx.doi.org/10.1117/12.917717>.
- Xu L., Li J., Brenning A. (2014) - *A comparative study of different classification techniques for marine oil spill identification using RADARSAT-1 imagery*. Remote Sensing of Environment, 141: 14-23. doi: <http://dx.doi.org/10.1016/j.rse.2013.10.012>.
- Zengeya F.M., Mutanga O., Murwira A. (2012) - *Linking remotely sensed forage quality estimates from worldview-2 multispectral data with cattle distribution in a savanna landscape*. International Journal of Applied Earth Observation and Geoinformation, pp.513-524. doi: <http://dx.doi.org/10.1016/j.jag.2012.07.008>.
- Zhan Q., Molenaar M., Tempfli K., Shi W. (2005) - *Quality assessment for geo-spatial objects derived from remotely sensed data*. International Journal of Remote Sensing, 26 (14): 2953-2974. doi: <https://doi.org/10.1080/01431160500057764>.

Zhuang W., Mountrakis G. (2014) - *An accurate and computationally efficient algorithm for ground peak identification in large footprint waveform LiDAR data*. ISPRS Journal of Photogrammetry and Remote Sensing, 95: 81-92. doi: <https://doi.org/10.1016/j.isprsjprs.2014.06.004>.

© 2016 by the authors; licensee Italian Society of Remote Sensing (AIT). This article is an open access article distributed under the terms and conditions of the Creative Commons Attribution license (<http://creativecommons.org/licenses/by/4.0/>).